Human Cystathionine β-Synthase Is a Heme Sensor Protein. Evidence That the Redox Sensor Is Heme and Not the Vicinal Cysteines in the CXXC Motif Seen in the Crystal Structure of the Truncated Enzyme[†,⊥]

Shinichi Taoka,[‡,§] Bryan W. Lepore,[‡,||] Ömer Kabil,[§] Sunil Ojha,[§] Dagmar Ringe,*[,||] and Ruma Banerjee*[,§]

Biochemistry Department, University of Nebraska, Lincoln, Nebraska 68588-0664, and Department of Chemistry and Biochemistry and Program in Bioorganic Chemistry, Rosenstiel Basic Medical Sciences Research Center, Brandeis University, Waltham, Massachusetts 02254-9110

Received April 30, 2002

ABSTRACT: Elevated levels of homocysteine, a sulfur-containing amino acid, are correlated with increased risk for cardiovascular diseases and Alzheimers disease and with neural tube defects. The only route for the catabolic removal of homocysteine in mammals begins with the pyridoxal phosphate- (PLP-) dependent β-replacement reaction catalyzed by cystathionine β-synthase. The enzyme has a b-type heme with unusual spectroscopic properties but as yet unknown function. The human enzyme has a modular organization and can be cleaved into an N-terminal catalytic core, which retains both the heme and PLP-binding sites and is highly active, and a C-terminal regulatory domain, where the allosteric activator *S*-adenosylmethionine is presumed to bind. Studies with the isolated recombinant enzyme and in transformed human liver cells indicate that the enzyme is ∼2-fold more active under oxidizing conditions. In addition to heme, the enzyme contains a CXXC oxidoreductase motif that could, in principle, be involved in redox sensing. In this study, we have examined the role of heme versus the vicinal thiols in modulating the redox responsiveness of the enzyme. Deletion of the heme domain leads to loss of redox sensitivity. In contrast, substitution of either cysteine with a non-redox-active amino acid does not affect the responsiveness of the enzyme to reductants. We also report the crystal structure of the catalytic core of the enzyme in which the vicinal cysteines are reduced without any discernible differences in the remainder of the protein. The structure of the catalytic core is compared to those of other members of the fold II family of PLP-dependent enzymes and provides insights into active site residues that may be important in interacting with the substrates and intermediates.

Cystathionine β-synthase found in mammals is a unique heme protein that catalyzes a pyridoxal phosphate- (PLP-)[1] dependent condensation of serine and homocysteine to give cystathionine. It represents one of two major pathways for clearance of intracellular homocysteine, which is generated by the hydrolysis of AdoHcy, the product of AdoMet-dependent methyltransferases (Figure 1). Elevated levels of homocysteine are correlated with cardiovascular diseases, neural tube defects, and Alzheimer's disease (*1*−*3*). Inborn errors of metabolism resulting from mutations in cystathionine β-synthase represent the most common cause of hereditary hyperhomocysteinemia, and over 100 mutations have been described in this gene (*4*). Interestingly, pathogenic mutations in cystathionine β-synthase have pleiotropic clinical phenotypes in four major systems: the skeletal, vascular, ocular, and central nervous system are affected (*5*). An understanding of the structure and regulation of this enzyme

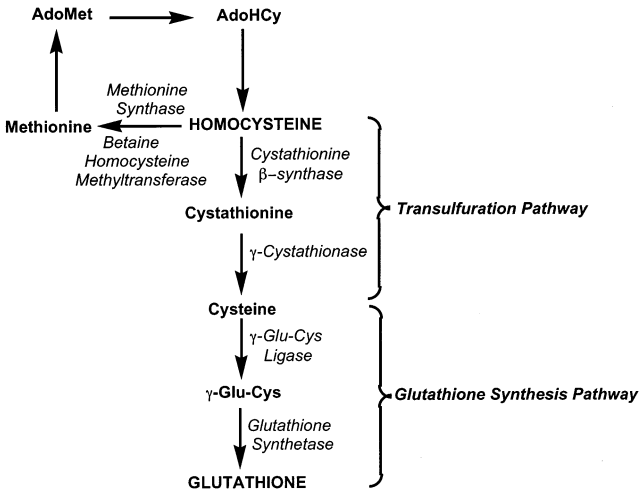

FIGURE 1: The transsulfuration pathway connects the methionine cycle to cysteine and glutathione biosyntheses. Cystathionine β-synthase is a key junction enzyme, which commits homocysteine to cysteine synthesis.

[†] This work was supported in part by a grant from the National Institutes of Health (HL58984 to R.B.) and from the National Science Foundationan (DBI-9874458 to D.R). R.B. is an Established Investigator of the American Heart Association.

[⊥] Coordinates of the structure have been deposited in the Protein Data Bank (www.rcsb.org/pdb/) with accession code 1M54.

* Corresponding authors. E-mail: rbanerjee1@unl.edu and ringe@brandeis.edu.

[‡] These authors contributed equally to the significant aspects of this study.

[§] University of Nebraska.

[||] Brandeis University.

[1] Abbreviations: PLP, pyridoxal phosphate; AdoMet, *S*-adenosylmethionine; AdoHcy, *S*-adenosylhomocysteine; NCS, noncrystallographic symmetry.

10.1021/bi026052d CCC: $22.00
Published on Web 07/25/2002

as well as its roles in these organ systems is essential for understanding the complex physiological manifestations of its dysfunction.

Human cystathionine β-synthase is composed of 63 kDa monomers that form oligomers that appear to represent aggregates of an α_4 structure (*6*, *7*). It has an N-terminal 66 amino acid extension where the heme is bound, which is missing from the homologous yeast enzyme (*8*, *9*). This is followed by a core domain that binds PLP and structurally resembles other members of the fold II family of PLP enzymes, viz., *O*-acetylserine sulfhydrylase and tryptophan synthase (*8*). The C-terminus of the protein constitutes the binding domain for AdoMet, an allosteric activator of the enzyme (*10*). Deletion of the C-terminal 143 residues results in a catalytic core, which is dimeric and retains high levels of enzyme activity but is unresponsive to AdoMet (*10*).

The role of PLP in this enzyme is easily rationalized on the basis of the chemical similarity to other β-replacement reactions catalyzed by PLP-dependent enzymes. In contrast, the role of the heme is not obvious, and several studies indicate that it may play a regulatory role (*6*, *11*). The heme is spectroscopically unusual (*11*−*13*) and is axially coordinated by residues C52 and H65 provided by the protein (*9*). Reduction of the heme results in a significant red shift in the Soret absorption band from 428 to 448 nm and is correlated with an ~2-fold decrease in the activity of the enzyme in vitro (*6*). While the magnitude of redox regulation of cystathionine β-synthase activity is modest, it should be noted that regulatory changes in the 1.5−3-fold range in mammalian housekeeping enzymes have physiologically significant effects (*14*).

The reaction catalyzed by cystathionine β-synthase represents the first committed step in the transsulfuration pathway that leads to the formation of cysteine from the essential amino acid, methionine (Figure 1). This pathway has a limited tissue distribution and appears to be present in organs that have high levels of glutathione, the major intracellular redox buffer. The limiting component in the synthesis of glutathione is believed to be cysteine, and the transsulfuration pathway provides an additional route for intracellular cysteine in tissues where the glutathione pool size, which can vary from 1 to 10 mM, is large. Studies with transformed human liver cells in culture (*15*) and with rat hepatocytes (*16*) have revealed that the transsulfuration pathway is a quantitatively significant contributor of intracellular cysteine and that approximately half of the cysteine in glutathione is derived via this pathway. Furthermore, flux of homocysteine through cystathionine β-synthase is responsive to oxidative stress in cultured cells (*15*). These observations underscore the importance of elucidating the molecular mechanism of the redox sensitivity of the enzyme to understand its role in modulating glutathione-dependent redox homeostasis (*15*).

In addition to the heme, the enzyme contains a CXXC motif that is surface exposed in the dimeric catalytic core of the enzyme (*8*). Although unusual for cytosolic enzymes because of the reducing environment (with an ~100:1 distribution of glutathione to glutathione disulfide in the liver), a reversible redox change in the vicinal cysteines involving a dithiol−disulfide equilibrium was suggested as an alternate redox sensing mechanism for the protein (*8*). In this study, we report that deletion of the heme-binding domain but not mutagenesis of the cysteines in the CXXC motif results in loss of redox sensitivity in cystathionine β-synthase. We also report the crystal structure of a truncated dimeric form of cystathionine β-synthase in which the vicinal cysteine residues are reduced and discuss active site models that contain bound intermediates.

MATERIALS AND METHODS

Materials. D,L-Homocysteine, dithionite, and L-cystathionine were purchased from Sigma. [^{14}C]Serine (158 mCi/mmol) was purchased from Amersham Pharmacia. The concentration of homocysteine was determined spectrophotometrically using Ellman's reagent (*17*). Pfu Turbo DNA polymerase was purchased from Stratagene.

Generation of Cystathionine β-Synthase Mutants. Pfu Turbo polymerase was employed for PCR, and the sequence of each of the final expression clones was verified by DNA sequence determination at the Genomics Core Facility at the University of Nebraska, Lincoln. The C272A and C274S mutants were generated using an overlapping PCR method. The following flanking primers were used in each case. The mutagenic primers for the two mutations were as follows: C272A sense, 5′-GGCCCCTGGATGCAGGATCATTGGGGTGGATCCC-3′; C272A antisense, GGGATCCACCCCAATGATCCTGCATCCAGGGGCC; C275S-sense, 5′-GAGAAGTGTCCTGGAAGCAGGATCATTGGGGTG; C275S-antisense, 5′-CACCCCAATGATCCTGCTTCCAGGACACTTCTC. The flanking primers used to generate both mutations were as follows: sense, 5′-TCCGCGTGGATCCCCGGAATTC; antisense, 5′-CAGTCACGATGCGGCCGCTCGA-3′. The resulting 2.4 kb fragment was digested with *Sal*I and ligated to the pGEX4T1 vector linearized with *Sal*I using T4 DNA Ligase (Life Technologies, Inc.). The mutations were confirmed by nucleotide sequencing.

Two deletion variants, one lacking the N-terminal heme domain (CBS-ΔN69) and a second lacking portions of the N- and C-terminal domains (CBS-ΔN43/ΔC143), were created by PCR from the parent pGEX4T1/hCBS plasmid (*18*). The Quick Change kit (Stragene) was employed for the CBS-ΔN69 construct using the following two primers: sense, 5′-CCCCACATCACCACA**GTCGAC**CGGCAAAATCTCCAAAAATCTTGCC-3′, and antisense, 5′-GGCAAGATTTTTGGAGATTTTGCCG**GTCGAC**TGTGGTGATGTGGGG-3′. The sequences in bold represent the *Sal*I site that was introduced in the primers and following PCR was used to generate a 2.2 kb fragment that was ligated to the pGEX4T1 vector also digested with *Sal*I. The sequence of the expression vector pCBS-ΔN69 was verified by nucleotide sequence determination.

Generation of the CBS-ΔN43/ΔC143 variant was accomplished in two stages. In the first, the N-terminal deletion was engineered into the parent pGEX4T1/hCBS plasmid using overlap extension PCR to generate an 880 base pair fragment containing a *Sph*I site 130 bases downstream of the ATG start codon in the parent plasmid. The following mutagenic primers were employed with the *Sph*I site depicted in bold: sense, 5′-GCCAAGGAGCCCCTGT**GCATGC**GGCCCGATGCTCCG, and antisense, 5′-CGGAGCATCGGGCC**GCATGC**ACAGGGGCTCCTTGGC. The following flanking primers were used: sense, 5′-TCCGCGTGGATCCCCGGAATTC-3′, and antisense, 5′-CGGGATCCACCCCAATGATCCTGC-3′.

The PCR product was cloned into the TA vector (Invitrogen) to give plasmid, pA, and digested with *Sph*I and *Xho*I (present in the vector) to give a 764 base pair fragment. The latter was ligated to the vector-bearing fragment resulting from digestion of the parent pGEX4T1/hCBS plasmid with the same enzymes. The resulting vector, designated pB, was digested with *Bbr*PI and *Sph*I, and the 297 base pair fragment in the resulting plasmid was exchanged with the corresponding fragment obtained from pGEXCBSN, which contains an insert carrying the ΔC143 deletion of cystathionine β-synthase (*18*). In this construct, pCBS-ΔN43/ΔC143, a new ATG start codon was introduced via the *Sph*I site and replaced the ATC encoding I44 in the parent plasmid.

Purification of Mutant Enzymes and Enzyme Assays. The deletion mutants, CBS-ΔN43ΔC143 and CBS-ΔN69, and the site-specific mutants, C272A and C275S, were expressed in and purified from *Escherichia coli* BL21 cells (Invitrogen). Expression of the CBS-ΔN69 mutant was performed at 15 °C because the protein was present predominantly in inclusion bodies at 25 °C. The recombinant enzymes were purified as described previously for the wild-type enzyme (*6*). Since the expression level of the C275S mutant was lower than that of the wild-type enzyme, it was purified via an additional step, i.e., chromatography on an HPLC gel filtration column (SEC-400 from Bio-Rad) eluted isocratically with 0.1 M Tris, pH 8.0, containing 0.15 N NaCl and 5 mM dithiothreitol at a flow rate of 0.75 mL min^{-1}.

Crystallization. Crystals of cystathionine β-synthase were grown using the hanging drop diffusion method from equal volumes of ∼45 mg/mL protein solution (in 0.1 M Tris-HCl, pH 8.0) and well solution (18−22% PEG 10K, 1 mM DTT, 0.1 M Tris-HCl, pH 8.0). Crystals grew as tetragonal blocks and shards approximately 0.2 mm × 0.3 mm × 0.5 mm at 25 °C within 4 days. Crystals were cryoprotected by gradually transferring them into a solution composed of 0.1 M Tris-HCl, pH 8.0, and 30% PEG 10K and subsequently freezing them in liquid nitrogen. Crystals were transported dry at liquid nitrogen temperature.

X-ray Diffraction Data Collection and Structure Determination. Data from crystals of CBS-ΔN43/ΔC143 were collected at beam line 14-BMD at BioCARS of the Advanced Photon Source (APS) at Argonne National Laboratory (ANL), using a Quantum 4 CCD and incident beam wavelengths of 1.7401 (iron edge) and 1.73720 (iron peak), at 100 K. The data sets were merged when iron in the heme was not located using MAD methods, which improved redundancy. Data were processed using the HKL package (*19*). Reduction of the data in higher symmetry space groups were attempted with Denzo and MOSFLM (*20*). Data collection statistics are listed in Table 1. The structure of cystathionine β-synthase was solved by molecular replacement using a dimer of 1JBQ as the starting model (*8*). Two of the top six solutions found with the program AMoRe (*21*, *22*) were used to define a reasonably packed tetramer. The hexamer was completed by running molecular replacement in the program CNS (*23*) by fixing the tetramer found with AMoRe while searching with a dimer. The *R*-factor of the initial solution was 47.4%, and the model occupies 45.5% of the unit cell. The *R*-factor dropped to 37.8% after rigid body refinement and continued to drop after simulated annealing. The molecules lie along a noncrystallographic 3_1 screw axis along the diagonal of the unit cell, of which the translational component gives rise to one strong and one weak off-origin peak in the native Patterson map. The 3-fold symmetry gives rise to a strong peak at 120° in the self-rotation map, while the 2-fold symmetry of the three dimers appears as three peaks at 180°. Upon inspection of the unit cell geometry, it was clear that it is not possible to choose a higher symmetry space group due to the angle that the molecular 3_1 screw axis makes with the faces of the cell. Electron density maps using the coefficients $2F_o - F_c$ calculated immediately after the molecular replacement showed that PLP was bound in all six subunits of the protein. The heme was less clear, but the remainder of the protein was reasonably defined, and density existed for residues which were left as alanine. Refinement using 6-fold NCS constraints relating all six subunits improved phases so that the heme became more evident. NCS constraints were imposed during initial refinement; then refinement was repeated without NCS constraints. A loop from residue 192 to residue 201 was omitted in all subunits due to lack of electron density, and the disulfide bond between residue 272 and residue 275 that existed in the 1JBQ starting model was observed to be reduced.

Table 1: Cystathionine β-Synthase Crystal and Data Set Statistics

space group	*P*1
V_M/molecules per asymmetric unit	2.63 Å Da^{-1}/6
a, *b*, *c* (Å)	85.8, 85.7, 97.1
α, β, γ (deg)	102.1, 101.5, 112.7
mosaicity (deg)	1.2−1.8
edge λ = 1.7401 Å	
total/unique no. of reflections	378472/53028
completeness: overall/highest shell (3.0−2.9 Å)	88.5%/ 88.5%
linear R_{merge}:[a] overall/highest shell (3.0−2.9 Å)	13.3%/41.7%
peak λ = 1.7372 Å	
total/unique no. of reflections	477536 /59297
completeness: overall/highest shell (2.9−2.8 Å)	90.4%/85.8%
linear R_{merge}:[a] overall/highest shell (2.9−2.8 Å)	14.8%/51.0%
merged peak and edge data set statistics	
total/unique no. of reflections	628994/53028
completeness: overall/highest shell (3.0−2.9 Å)	93.8%/93.2%
linear R_{merge}:[a] overall/highest shell (3.0−2.9 Å)	14.0%/45.9%
refinement statistics	
resolution range	50−2.9 Å
no. of reflections	628994
no. of unique reflections	53028
no. of reflections in test set	8143 (7.7% of unique reflections)
R_{cryst}[b]/R_{free}[c]	25.9%/34.8%
no. of atoms[d]	
protein	15840
ligands	360
metals	6
water	104
RMSD from ideal values[d]	
bond length	0.011 Å
bond angle	2.1°
dihedral angles	23.5°
improper torsion angles	1.18°

[a] $R_{merge} = \sum I_{hkl}|\langle I_o\rangle - \langle I\rangle|/\sum I_{hkl}$. [b] $R_{cryst} = \sum_{hkl}||F_o| - |F_c||/\sum_{hkl}|F_o|$. [c] $R_{free} = \sum_{hkl}||F_o| - |F_c||/\sum_{hkl}|F_o|$, where *hkl* includes the test set. [d] Analyzed using xtal_submission.inp and model_statistics.inp from PDB submission sections of the CNS suite of programs and Moleman2 worldwide web server at http://xray.bmc.uu.se/cgi-bin/gerard/rama_server.pl.

RESULTS AND DISCUSSION

Cystathionine β-synthase is a unique PLP-dependent heme protein in which the role of the heme cofactor is poorly

understood. The heme is spectroscopically unusual, and perturbation of the heme environment is correlated with a decrease or loss of enzyme activity (*6*, *11*, *12*, *24*). Of the various perturbations that have been reported, redox change in the heme has the mildest effect, and heme reduction is correlated with an ~2-fold diminution in enzyme activity (*6*).

Mutations in the human enzyme are the single most common cause of hereditary hyperhomocysteinemia, and these mutations represent a road map provided by nature of residues that are functionally important. To interpret the functional and mutational data within a structural framework, a three-dimensional structure of the protein is essential. In this study, we report the crystal structure of the catalytic core of the protein and demonstrate that deletion of the heme domain but not mutagenesis of the cysteines in the CXXC motif in human cystathionine β-synthase is correlated with loss of redox sensitivity of its catalytic activity.

Crystal Structure of the Catalytic Core of Cystathionine β-Synthase. The three-dimensional structure of the catalytic core, CBS-ΔN43/ΔC143, was solved by molecular replacement, which yielded electron density that, although noisy, traced the protein clearly and continuously. Electron density for the cofactors appeared when they were left out of the model, indicating that the maps were useful to build into. The noise level of the maps reflects the poor quality of the crystals, which could arise either from the weak intermolecular contacts or from a highly dynamic protein.

Cystathionine β-synthase adopts the overall fold of the tryptophan synthase family of PLP enzymes. The six three-dimensional structures currently known for this fold type are tryptophan synthase (2WSY), *O*-acetylserine sulfhydrylase (cysteine synthase, 1OAS), threonine synthase (1E5X), threonine deaminase (1TDJ), aminocyclopropanecarboxylate deaminase (1F2D), and cystathionine β-synthase (1JBQ), and the structures of all six have been determined by X-ray crystallography. Each of these enzymes holds PLP with the same absolute stereochemistry with the exception of threonine synthase, where this information is lacking because the structure lacked electron density for PLP.

The packing of the protein dimers to form a six-dimer unit is similar to the previously reported structure of cystathionine β-synthase (*8*). It is clear from the packing that two monomers associate to form dimers, in agreement with dynamic light scattering data obtained with this truncated form of cystathionine β-synthase (not shown). Each subunit of cystathionine β-synthase binds one PLP via C4A to K119, one heme with C52 and H65 serving as iron ligands, and all the residues that are in the vicinity of each cofactor are contributed by one monomer only. The distance from the heme to both the PLP and the vicinal thiols is approximately 20 Å (Figure 2). The hexamer that was used for refinement has two dimers surrounding a third dimer like calipers, such that the long axes of two dimers are perpendicular to the long axis of a third dimer. The dominant interaction between any two dimers is made by a strand from residues H66 to P78 and three loops spanning R132 to P134, Q365-G367, and P215-A216 and continues indefinitely. The closest distance between these four interacting groups of residues is approximately 5 Å and is composed mostly of hydrophobic residues. The interaction between dimers that are along this helical axis is much less extensive. One consequence of this

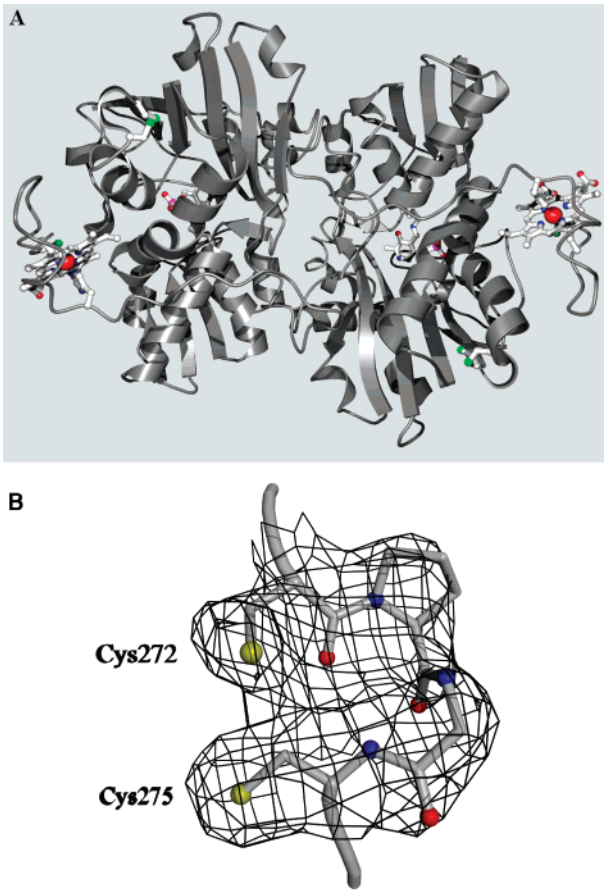

FIGURE 2: Overall structure of truncated cystathionine β-synthase and a close-up of the CXXC motif. (A) The dimer of human cystathionine β-synthase is represented as ribbons, while heme, PLP, and the CXXC motif are drawn as ball-and-stick models. Approximately 20 Å separate the heme, PLP, and CXXC motif from each other within each dimer, and the PLP is bound to the protein via K119 at C4A, also represented as a ball-and-stick model. The model was generated with Molscript and rendered in POV-ray (www.povray.org). (B) Close-up of the CXXC motif. The CPGC sequence of CBS is shown with representative $2mF_o - DF_c$ electron density contoured at 1.0σ. The model and electron density were generated with Povscript (D. Peisach and E. Peisach, personal communication) and rendered in POV-ray.

packing is that the hemes bound by subunits A and F are brought within 14 Å of each other; however, the physiological relevance, if any, of this packing is unknown.

The cystathionine β-synthase monomer contains three structurally conserved salt bridges that are also seen in the structures of other members of the fold II family of PLP enzymes. These are E239/K108, E110/R121, and E330/K359. The first two occur within hydrogen-bonding distance of each other forming a wall on the *si* face of the PLP behind the loop containing P375, and provide a link between the two subdomains of the monomer (Figure 3). In the primary sequence, three of the six residues, K108, E110, and R121, are less than 10 amino acids away from the PLP-lysine. Interestingly, R121 is a locus for pathogenic mutations correlated with hereditary hyperhomocysteinemia, and missense mutations converting this residue to leucine, cysteine, and histidine have been reported in patients (*4*). The proximity of these two salt bridges to the PLP suggests they are critical for maintenance of the organization of the monomer. These two bridges are also ~10 Å from the monomer−monomer interface, and the third conserved salt

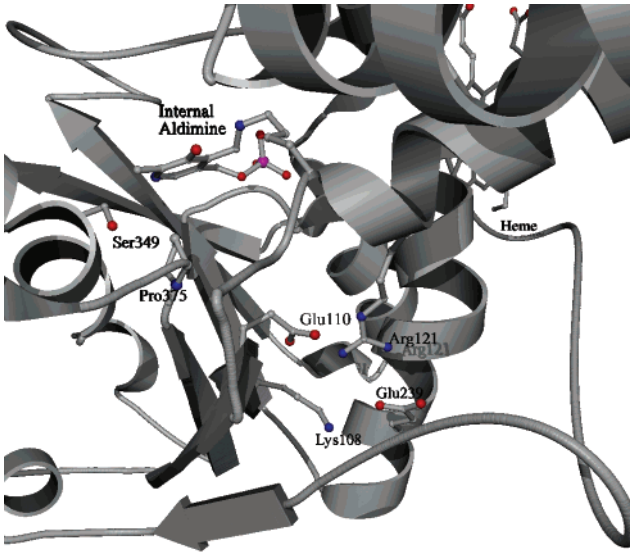

FIGURE 3: View of two salt bridges in cystathionine β-synthase that are absolutely conserved in the fold II family of PLP enzymes. The two salt bridges formed by E110−R121 and E239−K108 are found in close proximity within the monomer. A third structurally conserved salt bridge resides on a surface loop in the monomer between E330 and K359 and is not shown. The distance between R121 and E239 and between K108 and E110 is 3.2 and 5.3 Å, respectively. The salt bridges are approximately 15 Å from the *si* face of PLP, and three of the residues are found in the β-replacement enzyme PLP-binding motif, (see www.expasy.org/prosite/). P375 and S349 located near the pyridinium nitrogen are also shown, as is the heme in the background. The model was generated using Povscript and rendered in POV-ray.

bridge between E330 and K359 occurs on a loop on the surface of the monomer. E330 resides on a loop between a helix and sheet and forms a salt bridge to K359, which is found near the middle of the solvent-exposed side of a helix.

A loop on the *re* face of PLP helps to hold the cofactor in the protein and is held in place by a hydrogen bond from E304 to K384 (Figure 4). The appearance of one or more loops on the *re* face of PLP is another conserved feature of the β-replacement class of enzymes although this is currently unknown for threonine synthase because the structure lacked electron density for this region of the protein. Aminocyclopropane deaminase employs a combination of loops that is structurally distinct from the other enzymes to achieve the same end. The loops are always held in place by salt bridges reaching across the active site to the opposite side, and in tryptophan synthase, the aminoacrylate intermediate is within 4 Å of this loop.

The heme is cradled by an ~15 residue long N-terminal loop with C52 and H65 serving as iron ligands oriented perpendicular to the heme plane. The loop positions the heme at the distal ends of each dimer with an intersubunit heme distance of >40 Å. The intrasubunit distance between the heme and C4 of PLP and between the heme and the oxidoreductase motif is each 20 Å.

Cystathionine β-synthase contains an oxidoreductase motif, CXXC, which is conserved in other cystathionine β-synthase enzymes except for the yeast and *Dictyostelium* enzymes (*8*). The oxidoreductase motif in cystathionine β-synthase is comprised of residues C272, P273, G274, and C275 and is located on the surface of the distal ends of the dimers, between a helix and a β-strand (Figure 2A). Our structure shows that C272 and C275 are not covalently linked, presumably due to the presence of dithiothreitol in the crystallization medium (Figure 2B). A previous report of the structure of cystathionine β-synthase reported these cysteines to be oxidized (*8*). There is no significant structural change between these models of cystathionine β-synthase that can be attributed to oxidation state changes of the vicinal thiols. It is interesting to note that a mammalian PLP-dependent branched-chain aminotransferase contains redox-active vicinal thiols, although the functional significance of these thiols, if any, is unknown (*25*).

Analysis of the Active Site Structure of Cystathionine β-Synthase. PLP is held in the active site as an internal aldimine formed by the ϵ-nitrogen of K119 which extends from the back wall of the PLP-binding pocket (Figure 4). A number of loops that flank the cofactor position residues within hydrogen-bonding distance of the cofactor's heteroatoms, and all residues are contributed from the monomer to which the PLP is bound. S349 is positioned close to the pyridinium nitrogen of the cofactor, N149 is close to the phenolic oxygen of PLP, and the PLP phosphate is held near the monomer's center of mass by a loop containing G256,

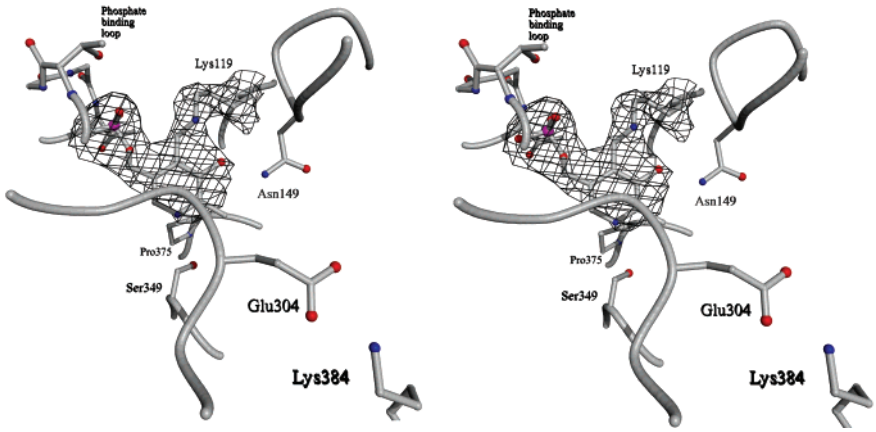

FIGURE 4: Active site structure of cystathionine β-synthase. The view is from the *re* face of the internal aldimine, showing representative $2mF_o - DF_c$ electron density. PLP forms an internal aldimine with Lys119. The flap in front of the PLP is held in place by a hydrogen bond from E304 to K384. N149 is hydrogen bonding to the phenolic oxygen of PLP, P375 approaches the pyridinium nitrogen of PLP from the *si* face of the cofactor, and S349 approaches from the *re* face. The phosphate-binding loop contains G256, T257, G258, and T260, which make hydrogen bonds to the phosphate oxygens via the backbone amides of the glycines, and threonine oxygens. The model and electron density were generated with Povscript and rendered in POV-ray.

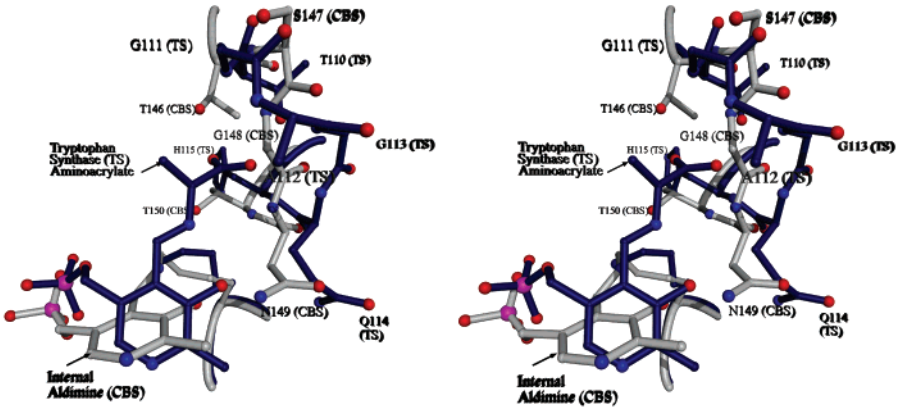

FIGURE 5: Overlay of cystathionine β-synthase (gray) and tryptophan synthase. A 1.7 Å RMSD overlay of tryptophan synthase aminoacrylate (gray, 1A5S) with cystathionine β-synthase (blue). The internal aldimine is shown attached to K119 in cystathionine β-synthase and is dissociated in the aminoacrylate form of tryptophan synthase. The PLP ring is tilted 15° in the aminoacrylate state compared to the internal aldimine. The labels CBS and TS denote residues from cystathionine β-synthase and from the tryptophan synthase aminoacrylate structure, respectively. The residue that is structurally equivalent to N149 in cystathionine β-synthase is Q114 in tryptophan synthase. Residues that are within hydrogen-bonding distance of the aminoacrylate in tryptophan synthase are shown in ball-and-stick representation.

T257, G258, G259, and T260. This loop is located at the N-terminus of an α-helix which points directly at the phosphate and is a conserved structural feature in all PLP-binding proteins whose folds are known. It is detectable by sequence alignment in all the enzymes with the β-replacement fold except for threonine synthase due to insertions which have caused the motif to appear earlier in the sequence.

Enzymes with the β-replacement fold, except threonine synthase, position an amido group within hydrogen-bonding distance of the phenolic oxygen of the PLP. This residue is an asparagine in four of the five enzymes [N149 in cystathionine β-synthase (Figure 4)], the exception being tryptophan synthase where it is a glutamine.

In this class of PLP enzymes, a polar residue (serine or threonine) is always found within hydrogen-bonding distance to the pyridinium nitrogen, either close to the back (*si* face) or the front (*re* face) of the cofactor, except in aminocyclopropane deaminase, where a glutamate is found directly below the PLP (*27*). Threonine synthase departs from this trend as a histidine is located on the *re* face. A closer look shows that the serines that form hydrogen bonds to the pyridinium nitrogen of the PLP in cystathionine β-synthase and in tryptophan synthase are in different positions in the two enzymes. In tryptophan synthase and threonine synthase (*26*), the serine approaches the cofactor from the *re* face, while in cystathionine β-synthase the hydrogen bond is made from the *si* face. The serine in tryptophan synthase was shown to be critical to the β-replacement functions of the enzyme by maintaining a low pK_a on the pyridinium nitrogen, as replacement by an acidic residue gave the enzyme spectral properties similar to aminotransferase and β-eliminase enzymes and increased the pK_a 2−5 units (*27*, *28*).

In cystathionine β-synthase and *O*-acetylserine sulfhydrylase a proline approches the pyridinium nitrogen from the *si* face of the PLP (*29*). In contrast, tryptophan synthase and threonine deaminase contain a serine on the *si* face in addition to the serine on the *re* face. Threonine synthase has a histidine on the *re* face. A structural alignment of the internal aldimine form of the enzymes reveals that both residues that approach the pyridinium nitrogen are found in moderately conserved regions of the protein. This suggests that the exact positioning of the serine in the active site is not significant to the β-replacement function of the enzymes, as long as a polar residue forms at least one hydrogen bond.

Two of the six β-replacement enzymes whose structures have been determined are known to catalyze reactions proceeding through an aminoacrylate intermediate. Both the human and yeast cystathionine β-synthase are shown to form an aminoacrylate intermediate in the presence of serine as detected by fluorescence and UV−visible absorption spectroscopy, respectively (*12*, *30*, *31*). It is likely that formation of the aminoacrylate intermediate is accompanied by a tilt of the PLP of approximately 15° about the axis roughly defined by the phosphate and methyl groups of the cofactor as seen in tryptophan synthase (*32*). Such a tilt would position the carboxylate group of the substrate within hydrogen-bonding distance of T146 and the backbone nitrogens of G148 and N149, as shown by a 1.7 Å RMSD overlay of the aminoacrylate form of tryptophan synthase with cystathionine β-synthase (Figure 5). Therefore, these residues may interact with the carboxylate of the substrate serine during the reaction catalyzed by cystathionine β-synthase. Homocysteine has been modeled into the rim of the active site in a location analogous to the entry port for indole in tryptophan synthase, and a number of polar and aromatic residues line the active site pocket that could facilitate the movement of homocysteine to the base of the active site pocket, where the presumed aminoacrylate species is bound (Figure 6).

The tryptophan synthase fold is frequently observed in conjunction with accessory proteins/domains. Of the six enzymes in this group, three (cystathionine β-synthase, threonine synthase, and threonine deaminase) contain additional domains at the C-terminus involved in regulation that do not contribute to the canonical tryptophan synthase fold. Tryptophan synthases from bacteria and higher plants exist as $\alpha_2\beta_2$ tetramers with α representing the regulatory subunit, while the yeast and mold enzymes are bifunctional. The N-termini are also highly variable in this enzyme class.

Redox Sensitivity of the CXXC Motif Mutants. Each of the two cysteine residues in the CXXC motif was mutated, and the redox sensitivity of the resulting enzymes was characterized. The UV−visible absorption properties of the mutant enzymes as isolated were very similar to that of wild-type cystathionine β-synthase with a Soret maximum at 428

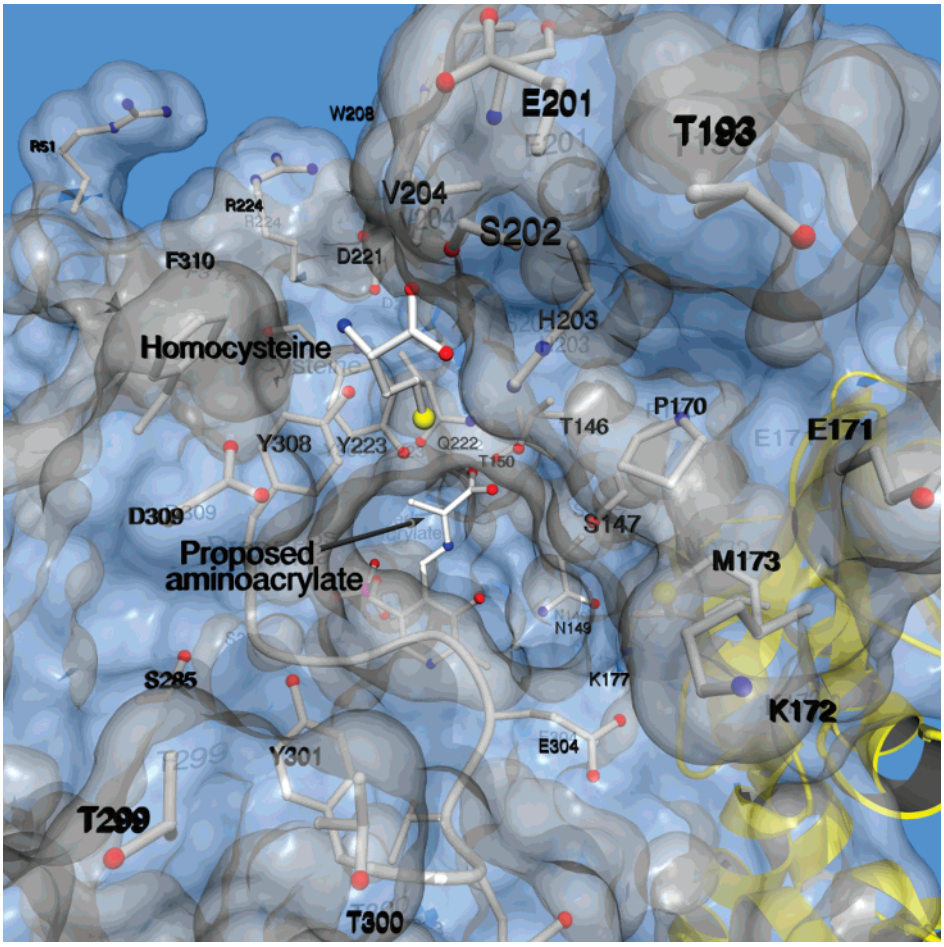

FIGURE 6: Surface representation of the active site entrance in cystathionine β-synthase. Homocysteine and the putative aminoacrylate intermediate are represented as ball-and-stick models with no surface, while the surface of cystathionine β-synthase is shown with residues lining the active site being labeled and depicted in ball-and-stick representation. Subunit B of the dimer is rendered in ribbons and colored yellow. The loop that holds the PLP in the active site is shown crossing over the pyridinium ring of PLP, which is located at the bottom of the pocket. Homocysteine has been modeled into the rim of the active site analogous to the putative entrance site of indole in tryptophan synthase, which uses a number of nonpolar aromatic amino acids in both its α and β subunits to guide indole toward the PLP-bound aminoacrylate. A number of polar residues line the mouth of the active site of cystathionine β-synthase, and homocysteine could approach from a number of angles. The surface was calculated using GRASP with a 1.4 Å probe radius and 1.5 grids/Å. The surface was input to povscript+ (T. Fenn, http://people.brandeis.edu/~fenn/povscript/povscript.php3), where it was oriented with the model, and then rendered with POV-ray.

nm and a broad $\alpha\beta$ absorption band centered at ~550 nm (not shown), consistent with the presence of heme in the ferric state. However, the heme content of both mutants was low as indicated by the ratio of the 280 nm (protein) to 428 nm (heme) absorptions, which is 0.92 in the wild-type enzyme and was 0.46 and 0.32 in the C272A and C275S mutants, respectively. The ~2-fold lower heme content of the mutant enzymes correlated with their ~2-fold lower specific activities as compared to the wild-type enzyme (Table 2). In addition, both mutants showed an ~2-fold higher activity in the presence of the allosteric effector, AdoMet, as observed with the wild-type enzyme (not shown).

Importantly, like the wild-type enzyme, which shows a 1.5−2-fold diminution in enzyme activity in the presence of reductants such as dithionite or titanium citrate, the C272A and C275S mutants displayed similar redox sensitivity (Table 2). These results exclude the role of the vicinal cysteines in the redox responsiveness of the human enzyme. Furthermore, these results are consistent with our previous observation that a two-electron reductant, viz., dithiothreitol, which should reduce an accessible disulfide but not the heme, does not affect the activity of the enzyme under anaerobic conditions (*6*). It should be noted that while the CXXC motif is solvent exposed in the structure of the truncated enzyme, its accessibility in the full-length enzyme is not known and may be significantly different.

Table 2: Relative Activities of Cystathionine β-Synthase Variants in the Presence and Absence of Reductant

enzyme	AdoMet	oxidized[a]	reduced	*x*-fold change
wild type	+	403 ± 75	235 ± 81	1.7
wild type	−	204 ± 22	146 ± 22	1.4
C272A	+	226 ± 15	151 ± 21	1.5
C275S	+	212 ± 13	114 ± 8	1.9
CBS-ΔN69	−	55 ± 7	50 ± 9	

[a] Enzyme activity was measured in the standard radioactive assay under anaerobic conditions in the presence (reduced) or absence (oxidized) of 1 mM titanium citrate and is given in units of μmol of cystathionine formed min^{-1} (mg of protein)$^{-1}$ at 37 °C.

Redox Sensitivity of the ΔN69-Hemeless Variant of Human Cystathionine β-Synthase. Residues C52 and H65 serve as the axial ligands to the heme in cystathionine β-synthase (*9*). Deletion of the N-terminal heme-binding domain in the

ΔN69 variant resulted in enzyme that was devoid of heme but had stoichiometric PLP (Ojha and Banerjee, unpublished results). The enzyme retained significant catalytic activity, representing ~27% of that observed with the full-length enzyme. However, in contrast to the wild-type enzyme and the CXXC motif mutants, the activity of the ΔN69 variant was insensitive to the presence of the low-potential reductant, dithionite (Table 2). Thus, the loss of heme is correlated with the loss of redox sensitivity in the human enzyme and provides strong evidence for the role of heme as a redox sensor in this protein. Heme sensor proteins are a newly recognized class of heme proteins described largely in bacteria (*33*−*38*). To our knowledge, this is the first example of a human heme sensor protein in which the redox state of the heme modulates catalytic activity.

Conclusions. In summary, our data provide compelling evidence that the redox sensitivity previously reported for human cystathionine β-synthase (*6*) is modulated by the presence of the redox cofactor, heme, rather than the CXXC oxidoreductase motif, which is present in the enzyme. The structure of the dimeric catalytic core reported here reveals the presence of the vicinal cysteines in the reduced state and no discernible differences from the structure in which the cysteines are oxidized (*8*). Models based on the structure of tryptophan synthase containing PLP-bound intermediates provide insights into residues that may be important for substrate binding and catalysis in human cystathionine β-synthase.

ACKNOWLEDGMENT

The authors thank Jim Clifton for assistance with molecular replacement using *O*-acetylserine sulfhydrylase and tryptophan synthase as search models and Greg Petsko for helpful advice.

REFERENCES

1. Refsum, H., Ueland, P. M., Nygard, O., and Vollset, S. E. (1998) *Annu. Rev. Med. 49*, 31−62.
2. Mills, J. L., McPartlin, J. M., Kirke, P. N., Lee, Y. J., Conle, M. R., and Weir, D. G. (1995) *Lancet 345*, 149−151.
3. Clarke, R., Smith, A. D., Jobst, K. A., Refsum, H., Sutton, L., and Ueland, P. M. (1998) *Arch. Neurol. 55*, 1449−1455.
4. Kraus, J. P., Janosik, M., Kozich, V., Mandell, R., Shih, V., Sperandeo, M. P., Sebastio, G., de Franchis, R., Andria, G., Kluijtmans, L. A., Blom, H., Boers, G. H., Gordon, R. B., Kamoun, P., Tsai, M. Y., Kruger, W. D., Koch, H. G., Ohura, T., and Gaustadnes, M. (1999) *Hum. Mutat. 13*, 362−375.
5. Mudd, S. H., Levy, H. L., and Skovby, F. (1995) *The metabolic and molecular basis of inherited diseases* (Scriver, C. R., Beaudet, A. L., Sly, W. S., and Valle, D., Eds.) McGraw-Hill, New York.
6. Taoka, S., Ohja, S., Shan, X., Kruger, W. D., and Banerjee, R. (1998) *J. Biol. Chem. 273*, 25179−25184.
7. Janosik, M., Kery, V., Gaustadnes, M., Maclean, K. N., and Kraus, J. P. (2001) *Biochemistry 40*, 10625−10633.
8. Meier, M., Janosik, M., Kery, V., Kraus, J. P., and Burkhard, P. (2001) *EMBO J. 20*, 3910−3916.
9. Ojha, S., Wu, J., LoBrutto, R., and Banerjee, R. (2002) *Biochemistry 41*, 4649−4654.
10. Taoka, S., Widjaja, L., and Banerjee, R. (1999) *Biochemistry 38*, 13155−13161.
11. Taoka, S., and Banerjee, R. (2001) *J. Inorg. Biochem. 87*, 245−251.
12. Taoka, S., West, M., and Banerjee, R. (1999) *Biochemistry 38*, 2738−2744.
13. Ojha, S., Hwang, J., Kabil, O., Penner-Hahn, J. E., and Banerjee, R. (2000) *Biochemistry 39*, 10542−10547.
14. Lee, C.-K., Klopp, R. G., Weindruch, R., and Prolla, T. A. (1999) *Science 285*, 1390−1393.
15. Mosharov, E., Cranford, M. R., and Banerjee, R. (2000) *Biochemistry 39*, 13005−13011.
16. Beatty, P. W., and Reed, D. J. (1980) *Arch. Biochem. Biophys. 204*, 80−87.
17. Ellman, G. L. (1959) *Arch. Biochem. Biophys 82*, 70−77.
18. Shan, X., and Kruger, W. D. (1998) *Nat. Genet. 19*, 91−93.
19. Otwinowski, Z., and Minor, W. (1997) *Methods Enzymol. 276*, 307−326.
20. Leslie, A. G. W. (1991) *Molecular data processing. Crystallographic computing 5: From chemistry to biology* (Moras, D., Podjarny, A. D., and Thierry, J.-C., Eds.) Oxford Science Publications, New York.
21. Navaza, J. (1994) *Acta Crystallogr. 50*, 157−163.
22. Collaborative Computational Project No. 4 (1994) *Acta Crystallogr. D50*, 760−763.
23. Brunger, A. T., Adams, P. D., Clore, G. M., DeLano, W. L., Gros, P., Grosse-Kunstleve, R. W., Jiang, J. S., Kuszewski, J., Nilges, M., Pannu, N. S., Read, R. J., Rice, L. M., Simonson, T., and Warren, G. L. (1998) *Acta Crystallogr. D: Biol. Crystallogr. 54*, 905−921.
24. Taoka, S., Green, E. L., Loehr, T. M., and Banerjee, R. (2001) *J. Inorg. Biochem. 87*, 253−259.
25. Yennawar, N., Dunbar, J., Conway, M., Hutson, S., and Farber, G. (2001) *Acta Crystallogr. D: Biol. Crystallogr. 57*, 506−515.
26. Thomazeau, K., Curien, G., Dumas, R., and Biou, V. (2001) *Protein Sci. 10*, 638−648.
27. Jhee, K. H., McPhie, P., Ro, H. S., and Miles, E. W. (1998) *Biochemistry 37*, 14591−14604.
28. Jhee, K. H., Yang, L. H., Ahmed, S. A., McPhie, P., Rowlett, R., and Miles, E. W. (1998) *J. Biol. Chem. 273*, 11417−11422.
29. Burkhard, P., Rao, G. S., Hohenester, E., Schnackerz, K. D., Cook, P. F., and Jansonius, J. N. (1998) *J. Mol. Biol. 283*, 121−133.
30. Jhee, K. H., Niks, D., McPhie, P., Dunn, M. F., and Miles, E. W. (2001) *Biochemistry 40*, 10873−10880.
31. Taoka, S., and Banerjee, R. (2002) *J. Biol. Chem. 277*, 22421−22425.
32. Schneider, G., Kack, H., and Lindqvist, Y. (2000) *Struct. Folding Des. 8*, R1−R6.
33. Gilles-Gonzalez, M. A., Gonzalez, G., and Perutz, M. F. (1994) *Biochemistry 33*, 8067−8073.
34. Delgado-Nixon, V. M., Gonzalez, G., and Gilles-Gonzalez, M. A. (2000) *Biochemistry 39*, 2685−2691.
35. Aono, S., Nakajima, H., Saito, K., and Okada, M. (1996) *Biochem. Biophys. Res. Commun. 228*, 752−756.
36. Shelver, D., Kerby, R. L., He, Y., and Roberts, G. P. (1997) *Proc. Natl. Acad. Sci. U.S.A. 94*, 11216−11220.
37. Chang, A. L., Tuckerman, J. R., Gonzalez, G., Mayer, R., Weinhouse, H., Volman, G., Amikam, D., Benziman, M., and Gilles-Gonzalez, M. A. (2001) *Biochemistry 40*, 3420−3426.
38. Sasakura, Y., Hirata, S., Sugiyama, S., Suzuki, S., Taguchi, S., Watanabe, M., Matsui, T., Sagami, I., and Shimizu, T. (2002) *J. Biol. Chem. 22*, 22.

BI026052D